DOI: 10.1002/adma.200701303

Nanolayered Carbon/Silica Superstructures via Organosilane Assembly

By *Huisheng Peng,* Yuntian Zhu, Dean E. Peterson,* and *Yunfeng Lu**

Carbon and silica play an important role in materials science due to their importance in both practical applications and academic research.[1] To synergistically utilize their interesting properties, attention has been increasingly paid to synthesizing carbon/silica hybrid nanocomposites with new interesting functionalities.[2] Various approaches have been extensively explored to achieve this goal. Among them, the most studied two methods are the incorporation of carbon with silica colloids or silica opals[3] and introduction of carbon into mesoporous silica.[4] Figure 1a shows the first synthetic approach using silica nanoparticles in two steps, i.e., mixture of silica nanoparticles and carbon precursors followed by carbonization of the introduced precursor at high temperatures. For this synthesis, the process is easy to operate and control, and the efficiency is typically high. However, the composites are not uniform; carbonization mainly produces amorphous carbon; both silica and carbon are not highly ordered; and it is difficult to tune the composite morphologies (normally films or powders, depending on the synthetic process). The second approach requires more complex operations (Fig. 1b): 1) formation of silica/surfactant nanocomposite materials by co-assembly of silicates and surfactants; 2) removal of surfactants by extraction or calcination; 3) incorporation of carbon precursors into the pores of the mesoporous silica materials; 4) carbonization of the carbon precursors at high temperatures. A main advantage using mesoporous silica is to synthesize carbon/silica composite materials with tunable mesostructures (lamellar, hexagonal, or cubic, depending on the used surfactants) and uniform compositions in the nano-scale. The limitations for the second fabrication include tedious procedures, production of amorphous carbon materials after carbonization, and uncontrolled morphologies of composite materials.

[*] Dr. H. Peng
Department of Chemical and Biomolecular Engineering,
Tulane University
New Orleans, LA 70118 (USA)
E-mail: hpeng@lanl.gov

Dr. H. Peng, Dr. Y. Zhu, Dr. D. E. Peterson
Los Alamos National Laboratory
Los Alamos, NM 87545 (USA)

Dr. Y. Lu
Department of Chemical and Biomolecular Engineering,
University of California
Los Angeles, CA 90095 (USA)
E-mail: luucla@ucla.edu

To summarize, the synthesized materials from above approaches show two common disadvantages. First, the carbon/silica composites are not conducting due to the formation of amorphous carbon, and they do not demonstrate good functionalities for potential applications in themselves. Therefore, the main focus is to remove silica using HF to produce porous carbon, which may be applied in water and air purification, separation, catalysis, and energy storage.[4] Second, films or powders are mainly produced by these two fabrications, depending on the synthetic process. It's difficult to synthesize silica/carbon composites with other tunable morphologies. Although templates, such as porous alumina films,[7] may be used to control their morphologies in some cases, the complex process severely decreases their efficiencies. Here we report the first example of synthesizing carbon/silica superstructures with controllable morphologies (tubes, fibers, or spheres) and sizes (from micro-scale to macroscopic) through a simpler process, i.e., self-directed assembly of an engineered bridged silsesquioxane, followed by carbonization of the building molecules. This novel synthesis requires only two steps with easy operation and high efficiency, without the use of any templates. Due to the sp^2-bonded carbon atoms in the hybrid structure, the derived carbon/silica superstructures demonstrated interesting electrical conductivity which exponentially increases with temperature. The tunable morphology and size as well as excellent electrical property make these superstructures very promising for many potential applications such as optoelectronic and sensing devices.

Self-assembly of bridged silsesquioxanes via sol-gel process has been extensively investigated to design and fabricate functional materials because of its simplicity.[8] A typical molecular structure for bridged silsesquioxanes is $(RO)_3$–Si–R′–Si–$(RO)_3$, where OR is a hydrolysable alkoxide group such as CH_3O– and CH_3CH_2O–, and R′ is a non-hydrolysable functional group such as phenyl, octyl, aminoalkyl, cyanoalkyl, thioloalkyl, epoxyl, vinyl, and conjugated diacetylenic groups.[5,8–11] By tuning noncovalent interactions among these building molecules, such as π–π interactions among the conjugated bridging organic R′ moieties, it is possible to precisely control the final assembled structure.[8b] One important type of R′ moieties are perylene derivatives. These derivatives have been widely studied not only because of their unique combination of optical, redox, and stability properties,[12] but also because of their interesting molecular structures, which may be engineered to assemble into desirable materials.[13]

ADVANCED MATERIALS

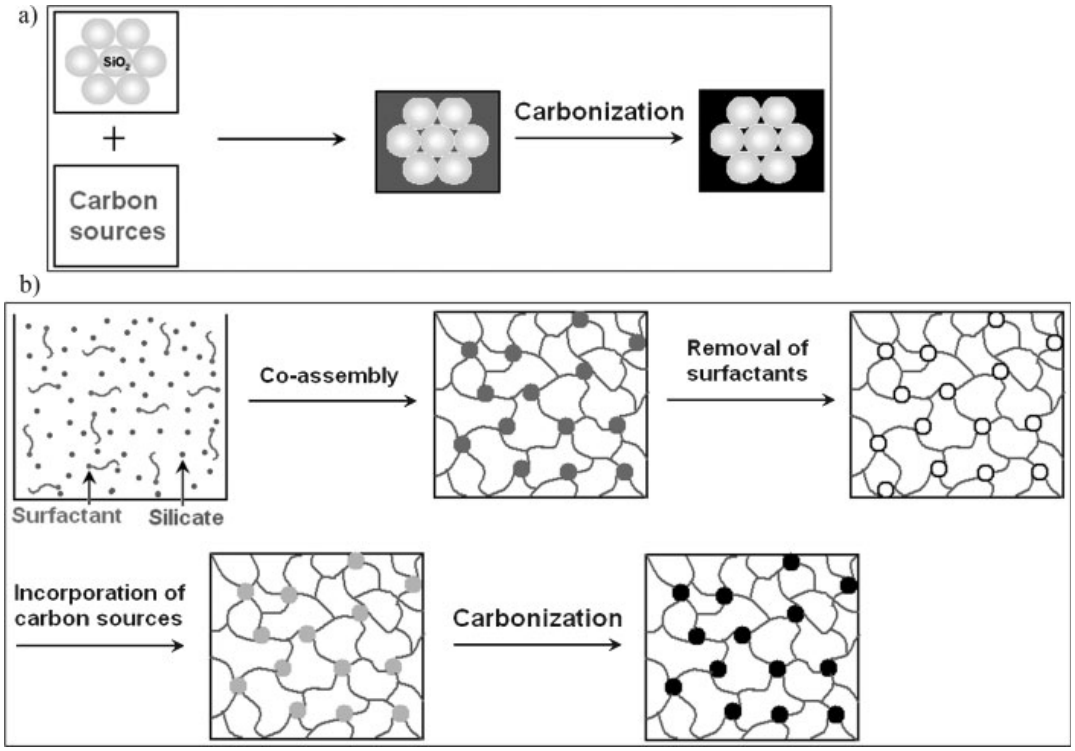

Figure 1. Schematic illustration of two main synthetic approaches to carbon/silica composite materials. a) Using silica colloids. b) Co-assembly of silicates and surfactants, followed by removal of surfactants, incorporation of carbon sources, and carbonization of designed carbon precursors, respectively. The carbon source can be small organic chemicals, polymers, or even polymeric micelles [5,6].

In this work, we introduced conjugated and disk-shaped perylene moieties into the R′ position to synthesize carbon/silica composite materials. As shown later, perylenediimide-bridged silsesquioxane (PDBS) building molecules demonstrated an interesting assembly behavior in THF/petroleum ether solutions. Specifically, they self-assembled into aggregates with tunable morphologies (tubes, fibers, or spheres) and sizes (micro-scale or macroscopic), depending on the experimental conditions. Similar to other organosilane assembly systems, the derived perylene/silica aggregates show a highly ordered lamellar mesostructure. Because of the multi-benzene structure of perylene moieties and mechanical stability of organosilane materials, PDBS assemblies can be easily carbonized to generate carbon/silica tubes, fibers, and spheres, providing a novel template approach to synthesize superstructured hybrid materials.

Scheme 1 shows the structure of PDBS building molecules, which are very stable in open air. PDBS was readily synthesized in one step from two commercially available precursors, (3-aminopropyl)triethoxysilane and 3,4,9,10-perylenetetracaboxylic dianhydride. More experimental details are described elsewhere.[14] To form the building assemblies, PDBS molecules were first dissolved in tetrahydrofuran (THF)/petroleum ether solutions, followed by evaporation of solvents.

Scheme 1. Chemical structure of the building PDBS molecule.

Two main factors that determine the assembly morphologies and sizes are the solution drying rate and PDBS concentration. The influence of solvent evaporation rate was quantitatively studied under an optical microscope, and was found to be more influential than the PDBS concentration. Tubes with uniform inner and outer diameters in the range of 3.7–7 μm and 5–10 μm, respectively, and length up to 1 mm were prepared by casting a PDBS THF/petroleum ether solution on glass substrates at room temperature, followed by air drying for ca. 5 min (Fig. 2a). The solution was prepared by mixing 1 unit of PDBS/THF and 5 unit of petroleum ether by volume, which yields a PDBS concentration of 8.3 mg mL^{-1}. Casting the same PDBS solution on glass substrates at higher temperatures of 65 °C and 90 °C and drying subsequently in ca. 10 and ca. 5 s, respectively, produced solid fibers with smaller diameters and lengths (Fig. 2b). As a comparison, if the solvent in the cast was evaporated over two weeks at room temperature, super-large fibers (Fig. 2c) with a diameter of 0.4 mm and length up to 1 cm were produced. Interestingly, these macroscopic fibers are composed of small tubes with sizes similar to those tubes shown in Figure 2a, suggesting two different levels of self-assembly.

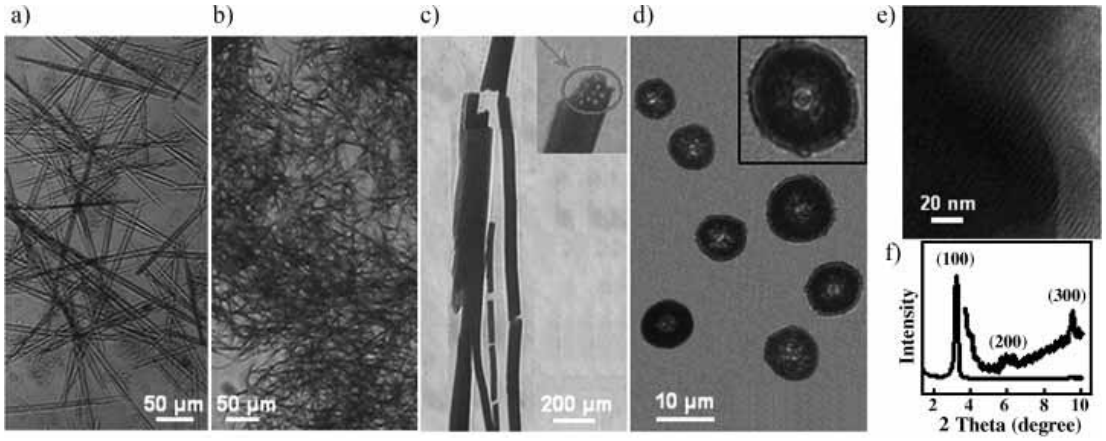

Figure 2. PDBS assemblies with tunable morphologies and sizes. a) Optical micrograph of tubes prepared by casting PDBS THF/petroleum ether solution (PDBS concentration = 8.3 mg mL^{-1}) on a glass substrate at room temperature. b) Optical micrograph of fibers prepared by casting PDBS THF/petroleum ether solution (PDBS concentration = 8.3 mg mL^{-1}) on a hot glass substrate with a temperature of ~65 °C. c) Optical micrograph of macroscopic fibers composed of a tubular structure produced by very slow evaporation (for ~ two weeks) of PDBS THF/petroleum ether solution (PDBS concentration = 8.3 mg mL^{-1}). d) Optical micrograph of hollow spheres after evaporation of PDBS THF/petroleum ether solution (PDBS concentration = 2.7–3.3 mg mL^{-1}) at room temperature. e) Typical transmission electron microscope image of tubular aggregates. f) Typical X-ray diffraction pattern of tubular aggregates with a d-spacing of 2.7 nm.

The initial PDBS concentration also plays an important role in morphology. Casting a solution with a lower PDBS concentration (3.3 mg mL^{-1}) on glass substrate at room temperature, for instance, produced hollow spheres after drying in ca. 5 min. Figure 2d shows a typical optical micrograph of hollow spheres with an average diameter of 10.9 μm and a polydispersity of 0.1, estimated from one hundred cases. For all of above aggregates, both transmission electron microscopy (TEM) and X-ray powder diffraction (XRD) (Fig. 2e and f) indicate a highly ordered lamellar structure with a d-spacing of 2.7 nm.

Based on molecular simulations,[14] we propose the following mechanism for the self-assembly of PDBS molecules (Fig. 3). At very dilute solutions, PDBS building blocks are molecularly distributed. With the evaporation of solvents, PDBS molecules first stack together to form small clusters. Further evaporation promotes progressive growth and aggregation of small clusters into assemblies with a highly ordered lamellar structure. The subsequent organization of clusters depends on the drying rate of solvent and initial PDBS concentration, which results in micro- or macro-assemblies with controlled morphologies. The

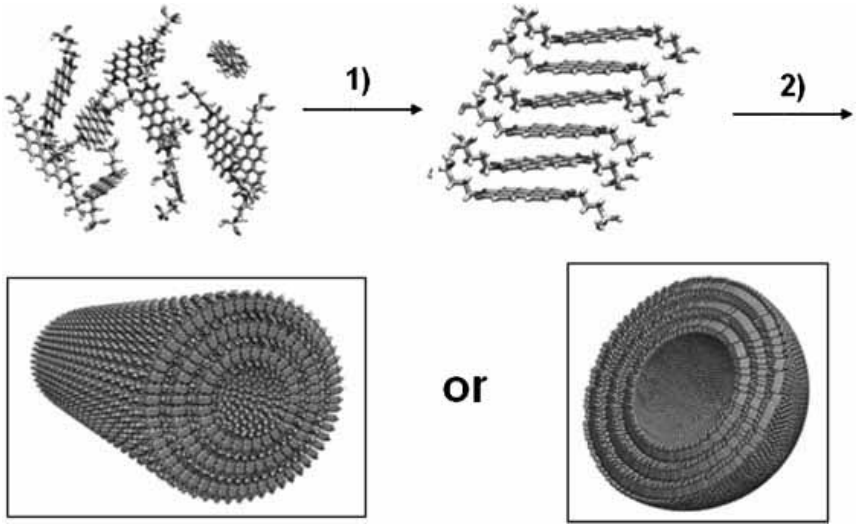

Figure 3. Schematic illustration of the lamellar structure of PDBS aggregates with various morphologies. The self-assembly steps include: 1) the formation of nanoscale PDBS clusters through π–π interactions among neighboring perylene moieties, 2) the growth and aggregation of the clusters to form tubular or spherical assemblies with a highly ordered lamellar structure.

ADVANCED MATERIALS

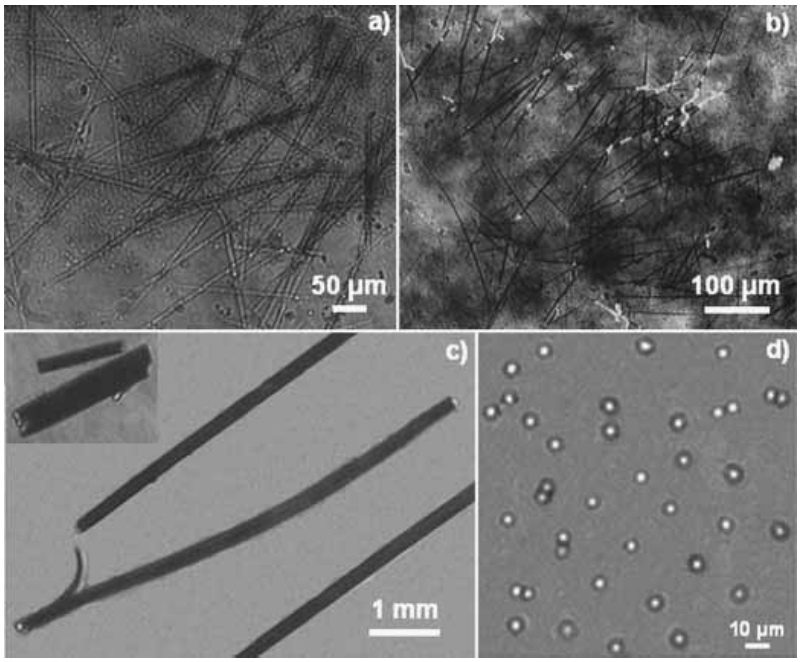

Figure 4. Optical micrographs of carbon/silica tubes (a), fibers (b), tubular fibers (c), and spheres (d).

hierarchical self-assembling process makes it possible to control the structure and composition of the final assemblies in the present system.

The building molecules with conjugated aromatic structures can be easily carbonized at high temperatures,[15] which provides for a practical method to produce carbon materials at large scale. Therefore, for bridged silsesquioxane systems, we hypothesize that hydrolysis and condensation reactions of the alkoxysilane substituents can create an inorganic silica framework that is covalently bonded with organic moieties, resulting in nanocomposites with greatly enhanced properties, e.g., mechanical stability. Therefore, tubular, fibril and spherical structures may be maintained after carbonizing PDBS assemblies.[16] This hypothesis has been verified in our experiments.

Figure 4 shows that perfect tubes, fibers and spheres were maintained after carbonization at 950 °C. In addition, the resultant carbon/silica tubes/fibers/spheres were also found to retain the layer-by-layer structure originated from PDBS building assemblies. Low angle XRD patterns confirmed their lamellar superstructure with a d-spacing of about 1.8 nm (Fig. 5a), smaller than that before carbonization. The d-spacing for the interlayer distance of carbon layers is ~4 Å. The successful carbonization is further characterized by ^{13}C NMR (Fig. 5b). The typical spectrum with a main peak at 118.5 ppm indicates that the carbon atoms are bonded in the form of sp^2. The ^{29}Si NMR spectrum (Fig. 5c) was used to investigate the state of Si atoms in the hybrid materials. A sharp peak at −108.5 ppm is ascribed to the Q^4 units [$Si(OSi)_4$]. The presence of Q^4 signals in the bulk state verified the formation of $(SiO_2)_x$ within the carbon matrix. Therefore, a carbon/silica superstructure was formed after the carbonization, and this superstructure acted as the basic unit building block to form various structural morphologies, including tubes, fibers and spheres.

The derived materials with the carbon/silica superstructure showed an excellent and tunable electronic property. We first compared the electrical conductivity of micrometer-sized tubes before and after carbonization at room temperature. Before carbonization, the conductivity of the tubes was less than 10^{-6} S cm^{-1}; after carbonization, the electrical conductivity increased dramatically to 1–40 S cm^{-1}. The improved electrical property of carbon/silica tubes was further characterized by testing their temperature dependence of conductivity using four-point contact method. Interestingly, the conductivity of the carbon/silica tubes increased exponentially with temperatures, following a relationship described by $\sigma = 6.88 \times 10^{-4}\ e^{(T/38.40)}$ (Fig. 5d). This temperature dependence of conductivity indicates a semiconducting behavior for the carbon/silica tubes.[17] It should be noted that the conductivity of these carbon/silica tubes increased by 40 times from 70 K to 433 K. As a comparison, the electric conductivity of multi-walled carbon nanotube sheets along the tube direction have a much smaller temperature dependence, which increased by only 50 % from 50 K to 400 K.[18] The huge dependence of conductivity on temperature may make the new carbon/silica superstructure promising for a wide variety of applications, such as optoelectronic and sensing devices.[19] Note that it is difficult to test the temperature dependence of conductivity for the tubes before carbonization.

In summary, this work demonstrated the first example to fabricate carbon/silica hybrid aggregates with a superstructure. The technique used in this study is self-assembly of perylene-

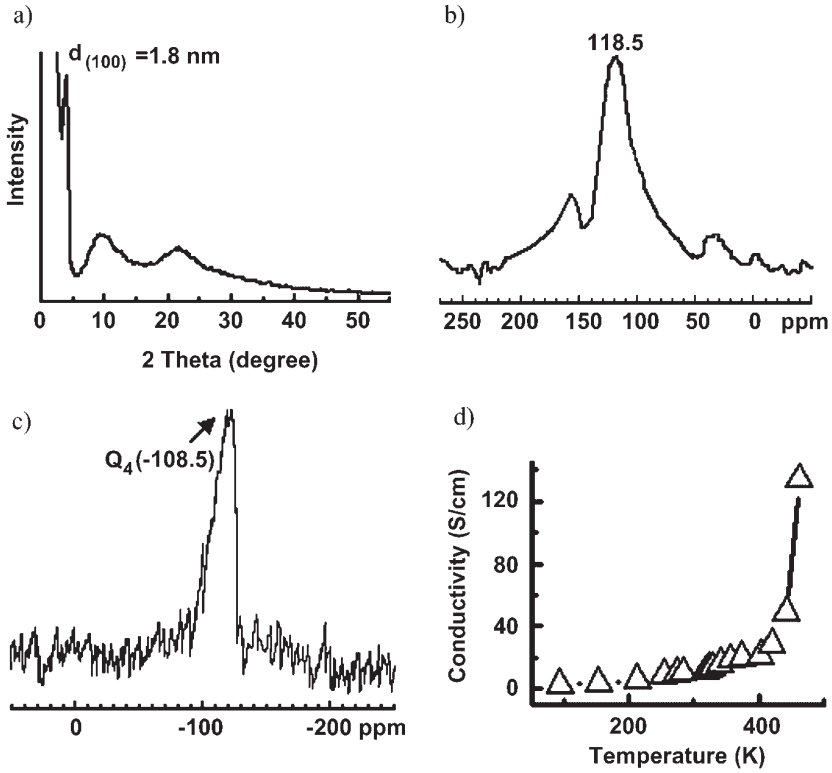

Figure 5. Structure and property characterizations of the derived carbon/silica tubes after carbonization at 950 °C. a) XRD; b) ^{13}C NMR; c) ^{29}Si NMR; d) electrical conductivity of a typical carbon/silica composite tube under different temperatures.

diimide-bridged silsesquioxane (PDBS) via an easy sol-gel process followed by carbonization at an elevated temperature. Aggregates with various morphologies, including tubes, fibers, and spheres, and sizes from micrometer to millimeter scale can be easily produced by varying the PDBS concentrations and drying speed. The electric conductivity of the carbon/silica aggregates demonstrated an exponential dependence on temperature. To the best of our knowledge, this phenomenon hasn't been observed in other carbon/silica hybrid systems. The novel behavior of such kind of carbon/silica aggregates and the simplicity of their synthesis make them promising in many device applications.

Experimental

To synthesize PDBS assemblies, a designed volume of petroleum ether (boiling point 60–80 °C) was added to a pre-prepared PDBS/THF solution at room temperature. The volume ratio of THF to petroleum ether was maintained at 1:5. The mixtures were then coated on glass substrates with temperatures ranging from 25 to 90 °C. Subsequent solvent evaporation at controlled rates resulted in the formation of assemblies with tubular, fibril, or spherical morphologies. Further hydrolysis and condensation of the triethoxysilane moieties within the resultant assemblies were conducted by exposing them to an acidic solution (pH = 1). The morphology study was conducted by fluorescence and visible microscopy (on an Olympus IMT-2 inverted microscope connected to a high-resolution monitor (SONY) and an S-VHS VCR through an Optronics CCD camera). The observations by fluorescence microscopy were conducted at $\lambda_{ex} = 490$ nm. The nanocomposites were further characterized using transmission electron microscope (JEOL 2010 microscope operated at 120 kV) and powder X-ray diffraction (XRD) patterns (Siemens D500 diffractometer operating at 40 kV, 30 mA, Cu Kα radiation, $\lambda = 0.15406$ nm). The electrical conductivity of micrometer-sized tubes was recorded over a frequency range of 10 to 1×10^7 Hz using a Solartron® 1260 gain phase analyzer. For this test, the temperature increases at a uniform rate of ca. 1.5 °C min^{-1} between two points. And at each temperature point, it was held for ca. 90 s to make sure that the superstructure temperature was stable.

Received: May 30, 2007
Revised: September 25, 2007

[1] H. Muller, P. Rehak, C. Jager, J. Hartmann, N. Meyer, S. Spange, *Adv. Mater.* **2000**, *12*, 1671.
[2] a) J. Rodriguez-Mirasol, T. Cordero, L. R. Radovic, J. J. Rodriguez, *Chem. Mater.* **1998**, *10*, 550. b) T. Kyotani, T. Nagai, S. Inoue, A. Tomita, *Chem. Mater.* **1997**, *9*, 609.
[3] a) S. Han, K. Sohn, T. Hyeon, *Chem. Mater.* **2000**, *12*, 3337. b) Z. Li, M. Jaroniec, *J. Am. Chem. Soc.* **2001**, *123*, 9208. c) A. A. Azkhidov, R. H. Baughman, Z. Iqbal, C. Cui, I. Khayrullin, S. O. Dantas, J. Marti, V. G.

ADVANCED MATERIALS

Ralchenko, *Science* **1998**, *282*, 897. d) J.-S. Yu, S. Kang, S. B. Yoon, G. Chai, *J. Am. Chem. Soc.* **2002**, *124*, 9382.
[4] a) Y. Deng, T. Yu, Y. Wan, Y. Shi, Y. Meng, D. Gu, L. Zhang, Y. Huang, C. Liu, X. Wu, D. Zhao, *J. Am. Chem. Soc.* **2007**, *129*, 1690. b) B.-H. Han, W. Zhou, A. Sayari, *J. Am. Chem. Soc.* **2003**, *125*, 3444. c) J. Kim, J. Lee, T. Hyeon, *Carbon* **2004**, *42*, 2711. d) Y. Mastai, S. Polarz, M. Antonietti, *Adv. Funct. Mater.* **2002**, *12*, 197.
[5] a) T. Asefa, M. J. MacLachlan, N. Coombs, G. A. Ozin, *Nature* **1999**, *402*, 867. b) T. Asefa, M. J. MacLachlan, H. Grondey, N. Coombs, G. A. Ozin, *Angew. Chem. Int. Ed.* **2000**, *39*, 1808.
[6] a) S. B. Yoon, J. Y. Kim, J.-S. Yu, *Chem. Commun.* **2002**, 1536. b) I. Moriguchi, Y. Koga, R. Matsukura, Y. Teraoka, M. Kodama, *Chem. Commun.* **2002**, 1844.
[7] a) W. Zhu, Y. Han, L. An, *Microporous Mesoporous Mater.* **2005**, *84*, 69. b) G. Kickelbick, *Small* **2005**, *1*, 168.
[8] a) H. Peng, J. Tang, L. Yang, J. Pang, H. S. Ashbaugh, C. J. Brinker, Z. Yang, Y. Lu, *J. Am. Chem. Soc.* **2006**, *128*, 5304. b) H. Peng, J. Tang, J. Pang, D. Chen, L. Yang, H. S. Ashbaugh, C. J. Brinker, Z. Yang, Y. Lu, *J. Am. Chem. Soc.* **2005**, *127*, 12782.
[9] a) J. J. E. Moreau, B. P. Pichon, M. Wong Chi Man, C. Bied, H. Pritzkow, J.-L. Bantignies, P. Dieudonne, J.-L. Sauvajol, *Angew. Chem. Int. Ed.* **2004**, *43*, 203. b) J. J. E. Moreau, L. Vellutini, M. Wong Chi Man, C. Bied, J.-L. Bantignies, P. Dieudonne, J.-L. Sauvajol, *J. Am. Chem. Soc.* **2001**, *123*, 7957. c) R. J. P. Corriu, J. J. E. Moreau, P. Thepot, M. Wong Chi Man, *Chem. Mater.* **1992**, *4*, 1217.
[10] a) M. P. Kapoor, Q. H. Yang, S. Inagaki, *J. Am. Chem. Soc.* **2002**, *124*, 15176. b) S. Inagaki, S. Guan, Y. Fukushima, T. Ohsuna, O. Terasaki, *J. Am. Chem. Soc.* **1999**, *121*, 9611.c) S. Guan, S. Inagaki, T. Ohsuna, O. Terasaki, *J. Am. Chem. Soc.* **2000**, *122*, 5660.
[11] A. Stein, B. J. Melde, R. C. Schroden, *Adv. Mater.* **2000**, *12*, 1403.
[12] a) K.-Y. Law, *Chem. Rev.* **1993**, *93*, 449. b) A. Yakimov, S. R. Forrest, *Appl. Phys. Lett.* **2002**, *80*, 1667. c) C. D. Dimitrakopoulos, P. R. L. Malenfact, *Adv. Mater.* **2002**, *14*, 99. d) F. Wurthner, *Chem. Commun.* **2004**, 1564.
[13] a) X. Zhang, Z. Chen, F. Wurthner, *J. Am. Chem. Soc.* **2007**, ASAP. b) A. P. H. J. Schenning, J. V. Herrikhuyzen, P. Jonkheijm, Z. Chen, F. Wurthner, E. W. Meijer, *J. Am. Chem. Soc.* **2002**, *124*, 10252. c) K. Balakrishnan, A. Datar, R. Oitker, H. Chen, J. Zuo, L. Zang, *J. Am. Chem. Soc.* **2005**, *127*, 10496. d) L. E. Sinks, B. Rybtchinski, M. Iimura, B. A. Jones, A. J. Goshe, X. Zuo, D. M. Tiede, X. Li, M. R. Wasielewski, *Chem. Mater.* **2005**, *17*, 6295. e) K. Baladrishnan, A. Datar, T. Naddo, J. Huang, R. Oitker, M. Yen, J. Zhao, L. Zang, *J. Am. Chem. Soc.* **2006**, *128*, 7390. f) M. J. Ahrens, L. E. Sinks, B. Rybtchinski, W. Liu, B. A. Jones, J. M. Giaimo, A. V. Gusev, A. J. Goshe, D. M. Tiede, M. R. Wasielewski, *J. Am. Chem. Soc.* **2004**, *126*, 8284. g) P. Jonkheijm, N. Stutzmann, Z. Chen, D. M. De Leeuw, E. W. Meijer, A. P. H. J. Schenning, F. Wurthner, *J. Am. Chem. Soc.* **2006**, *128*, 9535.
[14] Y. Luo, J. Lin, H. Duan, J. Zhang, C. Lin, *Chem. Mater.* **2005**, *17*, 2234.
[15] J. Pang, L. Yang, B. F. McCaughey, H. Peng, H. S. Ashbaugh, C. J. Brinker, Y. Lu, *J. Phys. Chem. B* **2006**, *110*, 7221.
[16] Z. Dai, L. Dahne, H. Mohwald, B. Tiersch, *Angew. Chem. Int. Ed.* **2002**, *41*, 4019.
[17] W. Zhou, J. Vavro, C. Guthy, K. I. Winey, J. E. Fischer, L. M. Ericson, S. Ramesh, R. Saini, V. A. Davis, C. Kittrell, M. Pasquali, R. H. Hauge, R. E. Smalley, *J. Appl. Phys.* **2004**, *95*, 649.
[18] M. Zhang, S. Fang, A. A. Zakhidov, S. B. Lee, A. E. Aliev, C. D. Williams, K. Atkinson, R. R. H. Baughman, *Science* **2005**, *309*, 1215.
[19] a) E. Bekyarova, M. E. Itkis, N. Cabrera, B. Zhao, A. Yu, J. Gao, R. C. Haddon, *J. Am. Chem. Soc.* **2005**, *127*, 5990. b) G. T. Kim, E. S. Choi, D. C. Kim, D. S. Suh, Y. W. Park, *Phys. Rev. B* **1998**, *58*, 16064.

